JOURNAL OF SOLID STATE CHEMISTRY 52, 281–291 (1984)

$Ba_{0.15}WO_3$: A Bronze with an Original Pentagonal Tunnel Structure

C. MICHEL, M. HERVIEU, R. J. D. TILLEY* AND B. RAVEAU

*Laboratoire de Cristallographie, Chimie et Physique des Solides, LA 251 ISMRA, Université, 14032 Caen Cedex, France, and *University of Bradford, Bradford, West Yorkshire BD7 1DP, England*

Received July 11, 1983; in revised form October 19, 1983

The structure of a new barium tungsten bronze, $Ba_{0.15}WO_3$, has been established by X-ray diffraction and high-resolution microscopy studies. This bronze is orthorhombic, space group *Pbm*2 or *Pbmm*, with $a = 8.859(3)$ Å, $b = 10.039(8)$ Å, and $c = 3.808(2)$ Å. The "WO_3" framework is built up from corner-sharing WO_6 octahedra forming pentagonal tunnels where the barium ions are located. Structural relationships with hexagonal tungsten bronze and tetragonal tungsten bronze structures are discussed.

Introduction

Oxygen tungsten bronzes A_xWO_3, in which A is characterized by a size greater or equal to that of potassium, exhibit two well-known structural types: the hexagonal tungsten bronze structure (HTB) for A = K, Rb, Tl, In, Cs (*1–9*), and the tetragonal tungsten bronze structure (TTB) for A = K, Ba (*10–13*). In addition, intergrowths of the HTB and WO_3 structures, called intergrowth tungsten bronzes (ITB), have been observed for smaller amounts of monovalent ions such as K^+, Rb^+, Tl^+, In^+, and Cs^+ (*12, 14, 15*). Recently, one of us (*13*) studied the formation of a series of barium tungsten bronzes: besides orthorhombic intergrowths which are ITB phases (to be published) and may be similar to the phases found in the Sn_xWO_3 and Pb_xWO_3 systems (*18–20*), a new phase was isolated with a composition close to $Ba_{0.15}WO_3$. The X-ray diffraction pattern of this phase was found to be similar to those of the niobate and tantalate $KCuM_3O_9$ (M = Nb, Ta) (*21*), recently studied in our laboratory for which a tunnel structure was proposed. The ability of WO_3 to form a tunnel framework in the presence of large ions suggested analogy with these latter materials. The results of an X-ray diffraction and electron microscopy study of this compound are reported below.

Experimental

Powder samples of $Ba_{0.15}WO_3$ were synthesized in vacuum-sealed quartz tubes from mixtures of $BaWO_4$, WO_3, and W in the correct ratios. The tubes were heated at 1000°C for several days, then quenched to room temperature.

Peak positions and intensities of X-ray diffraction patterns were measured from diffractograms registered with a Philips powder diffractometer using Cu$K\alpha$ radiation and a rotating sample holder. Calcula-

0022-4596/84 $3.00

tions of intensities were made using the scattering factors of ionic species from Cromer and Waber (*22*), corrected for the anomalous scattering (*23*).

The products of reaction were examined by transmission electron microscopy. For this purpose, the crystals were crushed in an agate mortar and dispersed in *n*-butanol. The fragments were collected on carbon-coated support grids and examined in a JEOL 100CX electron microscope, operating at 120 kV, using a goniometer stage (±60°) for electron diffraction study and a top entry goniometer (±10°) for high-resolution electron microscopy study. Only thin flakes projecting over holes in the support film were photographed, after having been aligned in such a way that the short *c* axis was parallel to the electron beam. All images were recorded by using an objective aperture with a radius of 0.42 $Å^{-1}$ in reciprocal space. A series of through-focus images was calculated with two programs, F. Coeff and Defect, developed by Skarnulius *et al.* (*24*); the parameters used in the calculation were incident beam convergence = 1×10^{-4} rad, spherical aberration constant C_s = 0.7 mm, depth of focus = 200 Å.

Structure Determination

The products of the reaction described under Experimental were dark blue and, as no other phases were present, were considered to have the stoichiometry of $Ba_{0.15}WO_3$. This phase crystallizes with an orthorhombic cell. The reflection conditions observed by electron diffraction, namely, $0kl$, $k = 2n$, lead to two possible space groups: *Pbm*2 (acentric) and *Pbmm* (centric). The X-ray patterns were indexed with the parameters $a = 8.859 \pm 0.003$ Å, $b = 10.039 \pm 0.008$ Å, and $c = 3.808 \pm 0.002$ Å. The experimental density ($d = 7.30$) agreed with six $Ba_{0.15}WO_3$ units per cell ($d_{calc.} = 7.43$).

The intensities of the first 59 peaks, i.e., 161 reflections, were measured. Twenty-eight intensities were of nonoverlapping reflections; these were corrected for PLG and multiplicity, and then introduced in a program for the calculation of the Patterson function. From the observed interatomic vectors, barium and tungsten atoms could be located in the 2(*f*), 2(*e*), and 4(*i*) sites of the *Pbmm* space groups (see Table I) with the following parameters: Ba—$x = 0.90$; $W_{(1)}$—$x = 0.60$; $W_{(2)}$—$x = 0.20$, $y = 0.41$. A calculation of intensities, including all the observed reflections, produced a discrepancy factor, $R = \Sigma|I_{obs} - I_{calc}|/\Sigma I_{obs}$, of 0.43.

The positions of the oxygen atoms were not easy to determine from the Fourier sections, owing to the low scattering factor of this atom compared to those of W and Ba. However, we can note that

—the coordination of tungsten is usually octahedral, with W–O distances close to 1.90 Å, which corresponds to half of the *c* parameter;

—the Ba–O distances are close to 2.80–2.90 Å in most of the known oxides.

TABLE I

VARIABLE PARAMETERS OBTAINED AFTER STRUCTURAL REFINEMENTS FOR THE OXIDE $Ba_{0.15}WO_3$ (SPACE GROUP *Pbmm*, $R = 0.056$)

Atom	Site	x	y	z	B (Å²)
Ba	2(f)[a]	0.920(1)	¼	½	0.5(3)
$W_{(1)}$	2(e)	0.5695(6)	¼	0	1.1(2)
$W_{(2)}$	4(i)	0.2054(4)	0.4393(4)	0	1.6(1)
$O_{(1)}$	2(f)	0.567(6)	¼	½	1.0[b]
$O_{(2)}$	4(j)	0.198(5)	0.408(5)	½	1.0
$O_{(3)}$	2(e)	0.171(6)	¼	0	1.0
$O_{(4)}$	2(a)	0	0	0	1.0
$O_{(5)}$	4(i)	0.432(4)	0.106(3)	0	1.0
$O_{(6)}$	4(i)	0.722(4)	0.123(3)	0	1.0

[a] This site is partially occupied by barium atoms (45%).

[b] For oxygen atoms, the *B* value is arbitrarily fixed at 1.0 Å².

In this way, the 18 oxygen atoms could be divided between six families (see Table I) compatible with the Fourier sections with the following approximate coordinates: $O_{(1)}$—x = 0.60; $O_{(2)}$—x = 0.20, y - 0.41; $O_{(3)}$—x = 0.12; $O_{(5)}$—x = 0.43, y = 0.13; $O_{(6)}$—x = 0.71, y = 0.11. The R factor value then fell to 0.38. The refinement of the structure was carried out with a program taking into account the overlapping peaks (*25*). The thermal factors of oxygen atoms were fixed at 1 Å^2, owing to the limited number of reflections relative to the number of variable parameters. A refinement of the atomic parameters of Ba and W led to an R value of 0.13 for the following values of the variables: Ba—x = 0.922; $W_{(1)}$—x = 0.573; $W_{(2)}$—x = 0.209, y = 0.445. Successive refinements of the atomic coordinates and of the isotropic thermal parameters (except for oxygen atoms), including all the intensities, lowered the R factor to 0.056. Values for the different variables are given in Table I. Refinement of barium occupancy led to the formula $Ba_{0.142}WO_3$ without any significant lowering of the R value; thus, the composition $Ba_{0.15}WO_3$ can be retained without major error.

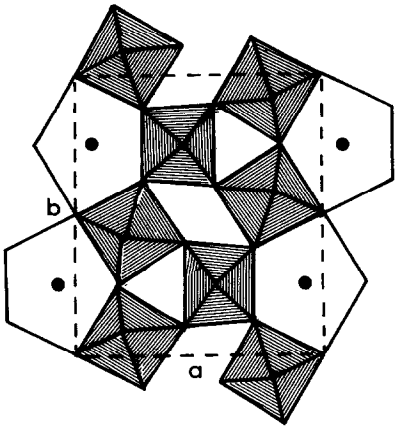

FIG. 1. Projection onto (001) of the $Ba_{0.15}WO_3$ structure.

Description of the Structure

The host lattice of this compound is built up from corner-sharing WO_6 octahedra which form pentagonal tunnels within which the barium ions are located (Fig. 1).

Two types of octahedra must be distinguished: the $W_{(1)}O_6$ which are almost regular and the $W_{(2)}O_6$ octahedra which are more distorted, as shown in Table II, where the different interatomic distances and angles are tabulated. The $W_{(1)}$–O_6 octahedra are characterized by two different "in-plane" W–O distances of 1.86 and 1.89 Å (mean value, 1.875 Å), while in the $W_{(2)}$–O_6 octahedra, four different distances, ranging from 1.92 to 2.06 (mean value, 1.965 Å) are observed. Barium atoms are surrounded by 15 oxygen atoms, 5 at the same level ($O_{(1)}$ and $O_{(2)}$), 5 at the upper level, and 5 at the lower level ($O_{(3)}$–$O_{(4)}$–$O_{(6)}$) which determine the pentagonal tunnel. The Ba–O distances range from 2.88 to 3.59 Å with a mean value of 3.10 Å. The angles between oxygen atoms forming the pentagonal section of the tunnel are in the range 94.5–117.8°; these values are different from those observed in tetragonal tungsten bronzes and are in consonance with a slight distortion of the tunnel.

The octahedral framework of $Ba_{0.15}WO_3$ consists of pentagonal rings of octahedra similar to those observed in the TTB structure (Fig. 2) forming pentagonal tunnels characterized by two angles close to 90° and two angles close to 120°. Along |010|, two adjacent pentagonal rings have two common octahedra so that the corresponding pentagonal tunnels share their corners along this direction. This structure can therefore be described as built up from identical ribbons of pentagonal rings running indefinitely along |010|, and sharing the corners of their octahedra along |100| (Fig. 2).

TABLE II

INTERATOMIC DISTANCES AND ANGLES

Distance (Å)		Angle (°)		Distance (Å)		Angle (°)	
		W1–O_6 octahedron					
$W_{(1)}$–$O_{(1)}$	1.904(1) × 2	$O_{(1)}$–$W_{(1)}$–$O_{(5)}$	89.6(8) × 4	$O_{(3)}$–$O_{(4)}$	2.93(3) × 1		
$W_{(1)}$–$O_{(5)}$	1.89 (3) × 2	$O_{(1)}$–$W_{(1)}$–$O_{(6)}$	90.5(9) × 4	$O_{(3)}$–$O_{(5)}$	2.73(6) × 1		
$W_{(1)}$–$O_{(6)}$	1.86 (3) × 2	$O_{(5)}$–$W_{(1)}$–$O_{(5)}$	99.8(9) × 1	$O_{(4)}$–$O_{(6)}$	2.75(3) × 1		
$O_{(1)}$–$O_{(5)}$	2.67 (3) × 4	$O_{(5)}$–$W_{(1)}$–$O_{(6)}$	86.8(9) × 2	$O_{(5)}$–$O_{(6)}$	2.57(5) × 1		
$O_{(1)}$–$O_{(6)}$	2.67 (3) × 4	$O_{(6)}$–$W_{(1)}$–$O_{(6)}$	86.7(9) × 1				
$O_{(5)}$–$O_{(5)}$	2.89 (4) × 1				BaO_{15} polyhedron		
$O_{(5)}$–$O_{(6)}$	2.57 (5) × 2			Ba–$O_{(1)}$	3.13(5) × 1	$O_{(1)}$–Ba–$O_{(2)}$	73.1(6) × 2
$O_{(6)}$–$O_{(6)}$	2.55 (5) × 1			Ba–$O_{(2)}$	2.93(5) × 2	$O_{(2)}$–Ba–$O_{(2)}$	74.1(8) × 2
				Ba–$O_{(2)}$	3.59(5) × 2	$O_{(2)}$–Ba–$O_{(2)}$	65.6(9) × 1
		W2–O_6 octahedron		Ba–$O_{(3)}$	2.93(4) × 2	$O_{(4)}$–$O_{(6)}$–$O_{(6)}$	116.6(9) × 2
$W_{(2)}$–$O_{(2)}$	1.931(8) × 2	$O_{(2)}$–$W_{(2)}$–$O_{(3)}$	80.4(1.0) × 2	Ba–$O_{(4)}$	3.229(2) × 4	$O_{(4)}$–$O_{(3)}$–$O_{(4)}$	117.8(5) × 1
$W_{(2)}$–$O_{(3)}$	1.925(9) × 1	$O_{(2)}$–$W_{(2)}$–$O_{(4)}$	91.1(9) × 2	Ba–$O_{(6)}$	2.88(2) × 4	$O_{(3)}$–$O_{(4)}$–$O_{(6)}$	94.5(6) × 2
$W_{(2)}$–$O_{(4)}$	1.919(4) × 1	$O_{(2)}$–$W_{(2)}$–$O_{(5)}$	89.8(1.1) × 2	$O_{(1)}$–$O_{(2)}$	4.01(5) × 4		
$W_{(2)}$–$O_{(5)}$	2.06 (3) × 1	$O_{(2)}$–$W_{(2)}$–$O_{(6)}$	99.5(1.1) × 2	$O_{(1)}$–$O_{(6)}$	2.67(3) × 8		
$W_{(2)}$–$O_{(6)}$	1.95 (3) × 1	$O_{(3)}$–$W_{(2)}$–$O_{(4)}$	99.4(5) × 1	$O_{(2)}$–$O_{(2)}$	3.96(6) × 2		
$O_{(2)}$–$O_{(3)}$	2.49 (3) × 2	$O_{(3)}$–$W_{(2)}$–$O_{(5)}$	86.4(9) × 1	$O_{(2)}$–$O_{(2)}$	3.17(7) × 2		
$O_{(2)}$–$O_{(4)}$	2.75 (3) × 2	$O_{(4)}$–$W_{(2)}$–$O_{(6)}$	90.7(6) × 1	$O_{(2)}$–$O_{(3)}$	2.49(3) × 4		
$O_{(2)}$–$O_{(5)}$	2.82 (3) × 2	$O_{(5)}$–$W_{(2)}$–$O_{(6)}$	83.5(9) × 1	$O_{(2)}$–$O_{(4)}$	2.75(3) × 8		
$O_{(2)}$–$O_{(6)}$	2.96 (4) × 2			$O_{(3)}$–$O_{(4)}$	2.93(3) × 2		
				$O_{(4)}$–$O_{(6)}$	2.75(3) × 2		
				$O_{(6)}$–$O_{(6)}$	2.55(5) × 1		
				$O_{(1)}$–$O_{(6)}$	2.67(3) × 8		

HREM Study

A high-resolution lattice image from a thin fragment of $Ba_{0.15}WO_3$ is reproduced in Fig. 3. The contrast consists of two types of ribbons of white patches lying alternately along the *b* axis: one of these ribbons is built up from the largest bright spots arranged in a zig-zag pattern, whereas in the other one, the weakest spots fall into line parallel to **b**. Geometric relations among white patches could be directly related to the structure, in that big white patches in the image correspond to half occupied tunnels of pentagonal cross section and the weakest ones, to the small empty rhombic tunnels.

Calculations were carried out using the

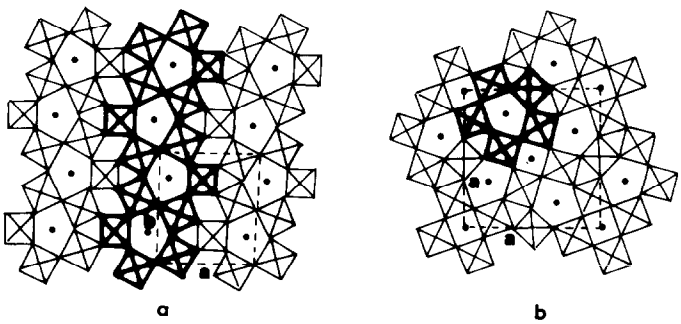

FIG. 2. (a) The $Ba_{0.15}WO_3$ structure described as built up from identical ribbons of pentagonal rings of octahedra. (b) The idealized TTB structure showing identical pentagonal rings of octahedra.

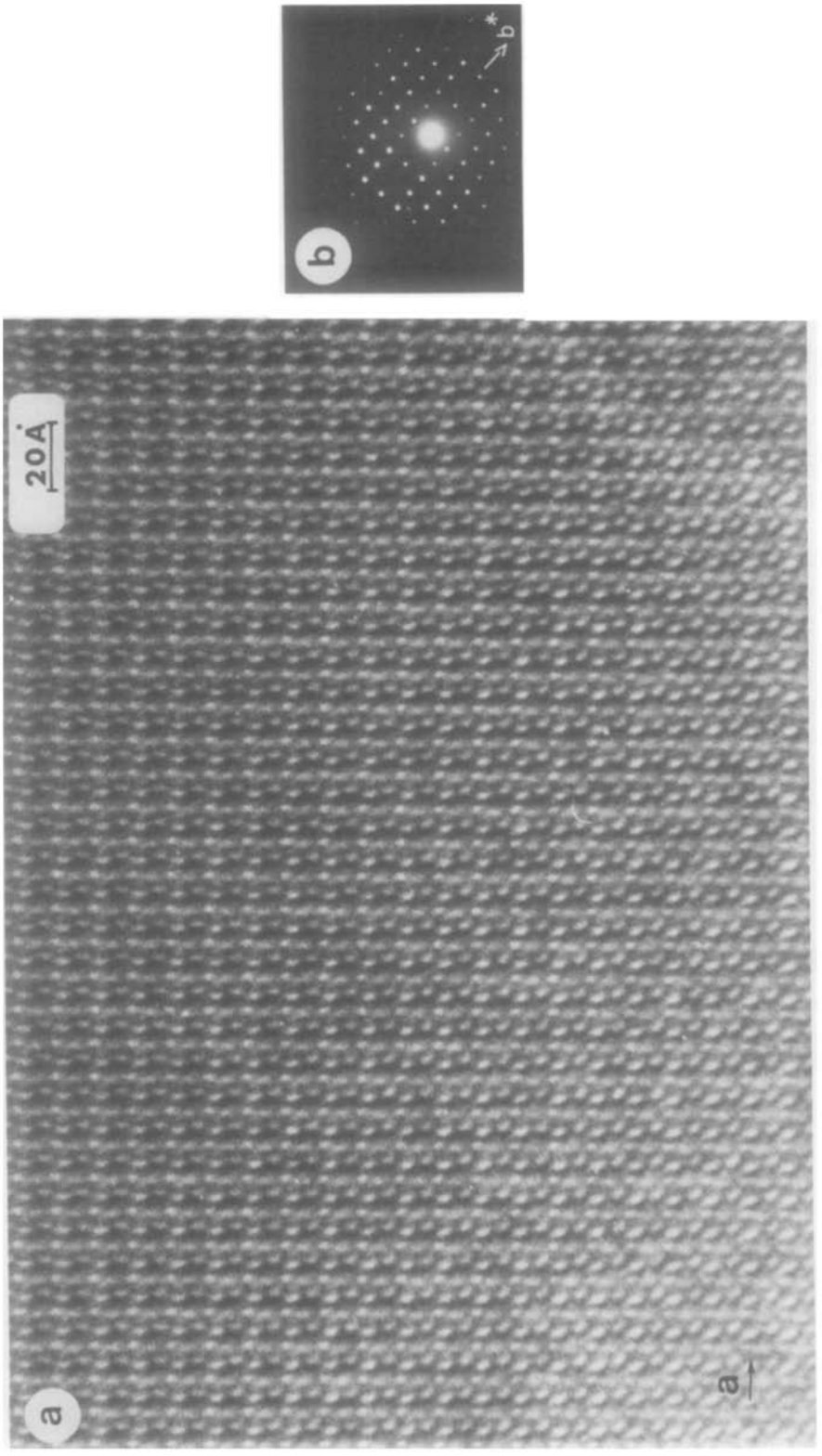

FIG. 3. (a) High-resolution lattice image and (b) electron diffraction pattern of a thin crystal of $Ba_{0.15}WO_3$.

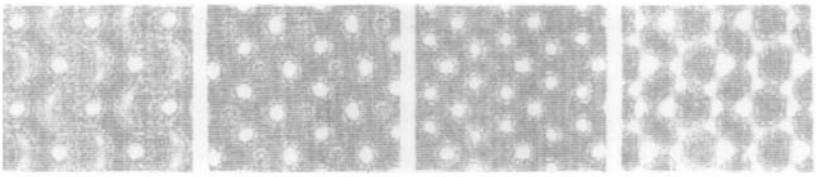

FIG. 4. Calculated through-focus images for a crystal having a thickness of five slices.

programs and the experimental parameters previously described. The slice thickness was taken to be equal to the short c axis (3.81 Å). Structural data used are those from the refined structure obtained by X-ray diffraction. Figure 4 shows the calculated through-focus images for a crystal having a thickness of five slices. For this model images at the optimum focus (−400 Å) show white spots, features in agreement with the experimental observations, and a reversed contrast for −800 Å. Similar sets of calculations were made in order to show the change of intensity of the spots for thicknesses of 10, 15, and 30 slices; these are shown in Fig. 5.

The experimental images and their theoretical calculations are in agreement and confirm our model of the structure.

Structural Relationships

These results show that the orthorhombic $Ba_{0.15}WO_3$ structure exhibits W_3O_{15} blocks resulting from the linkage of the pentagonal rings of octahedron ribbons along [100] similar to those already observed in the TTB structure (Fig. 2). However, contrary to TTB, $Ba_{0.15}WO_3$ does not exhibit the "W_5O_{24}" units (Fig. 6b) which correspond to the "association" of two M_3O_{15} blocks (Fig. 6a). It i important to note that such "W_5O_{24}" units can be obtained without changing the nature of the ribbons of pentagonal rings, as shown from the hypothetical structure in Fig. 7, in which these ribbons are absolutely identical to those observed in $Ba_{0.15}WO_3$; however, they are no longer independent, since two adjacent ribbons exhibit common octahedra. Such a framework forms pairs of pentagonal tunnels sharing one octahedron (Fig. 7), exactly as in the TTB structure.

The similarity of this hypothetical structure with that of $Ba_{0.15}WO_3$ suggests the possibility of formation of intergrowths of this structure with that found for $Ba_{0.15}WO_3$ (see Fig. 8), by changing the experimental conditions, and in particular, the temperature and time for synthesis. The HREM observations made on several crystals synthe-

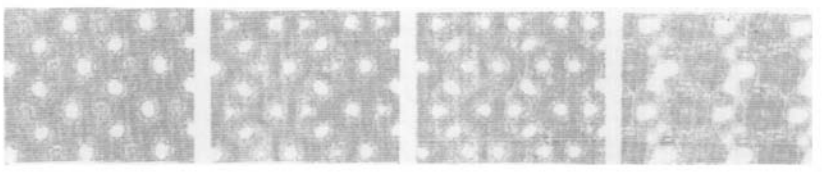

FIG. 5. Optimum-focus images calculated for various crystal thicknesses (one slice = 3.8 Å).

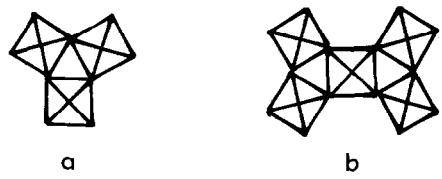

FIG. 6. (a) M_3O_{15} block observed in TTB and $Ba_{0.15}WO_3$. (b) M_5O_{24} block of the TTB resulting from the association of two M_3O_{15} blocks.

sized at 1100°C seem to confirm this point of view. In Fig. 9a we show the image of a crystal containing defects (arrows) running along [010]. Figure 9b corresponds to an enlargement of that defect and shows that the structure of the bulk is the same on both sides of the defect. The geometrical relations and the direction of the zig-zag ribbons of the pentagonal tunnels (enhanced by a black line on the micrograph) are in agreement with the idealized drawing of the defect which can be interpreted in terms of chemical twin defects of this type. The strongly disordered area reproduced in Fig. 10a could similarly be considered as a disordered intergrowth of $Ba_{0.15}WO_3$ and of the hypothetical structure $Ba_{0.20}WO_3$ (Fig.

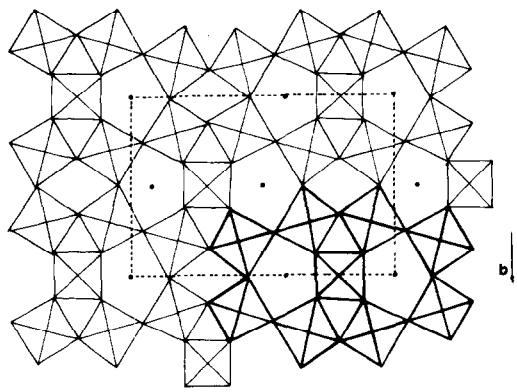

FIG. 7. $Ba_{0.20}WO_3$: hypothetical structure built up from ribbons of pentagonal rings of octahedra exhibiting common octahedra. The pair of pentagonal tunnels, similar to that observed in TTB, is enhanced by a heavy line.

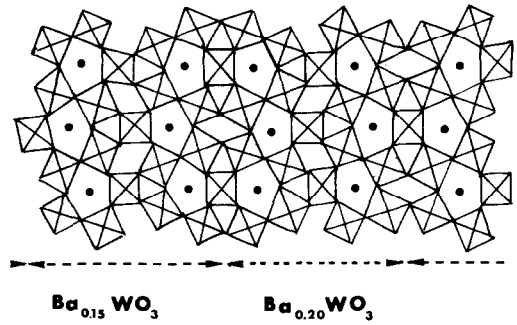

FIG. 8. Hypothetical intergrowth of $Ba_{0.15}WO_3$ and $Ba_{0.20}WO_3$.

8). Its electron diffraction pattern is characterized by streaking along the a^* axis (Fig. 10b).

The occupancy of the tunnels by barium ions is rather weak compared to that of $KCuTa_3O_9$ and $KCuNb_3O_9$ whose structures are similar (*21*). This low occupancy of the tunnels—less than half of the available sites—seems to be a characteristic of the Ba–W–O system, since the TTB structure which is formed in this system (*13*) is also barium deficient ($x = 0.20$–0.21). It is also remarkable that the maximum x value allowed by this framework is the same as that observed in HTB: $x = \frac{1}{3}$. In this respect the structural study of the potassium copper niobate (*21*) shows that both structures $Ba_{0.15}WO_3$ and $KCuM_3O_9$ (M = Nb–Ta) are closely related to the HTB.

Conclusion

$Ba_{0.15}WO_3$ exhibits an original pentagonal tunnel structure, closely related to the well-known TTB and HTB structures. The close relationships between these structures and the formation of defects corresponding to a different hypothetical structure open up a new direction for the establishment of non-stoichiometry in the A_xWO_3 bronzes; the possibility of intergrowths between these structures will be further investigated.

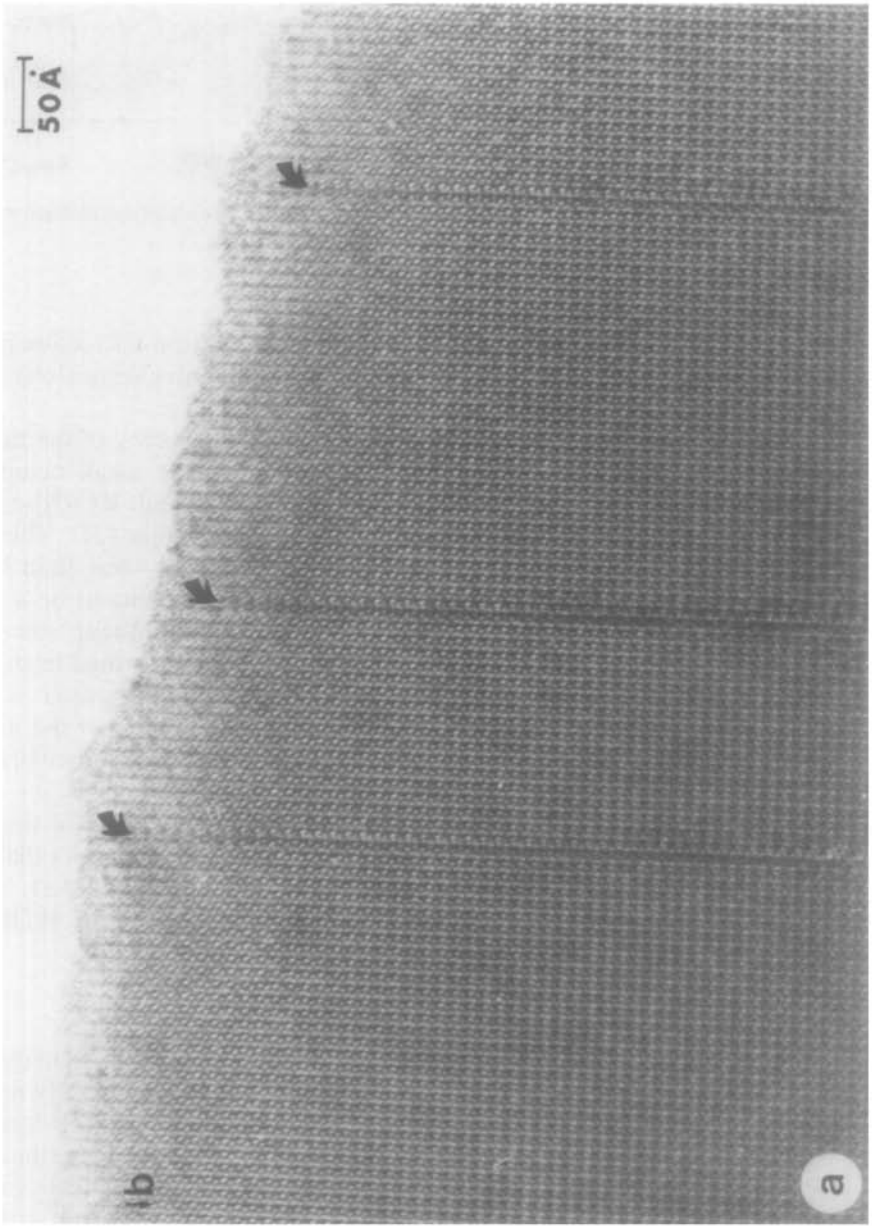
50 Å
b
a

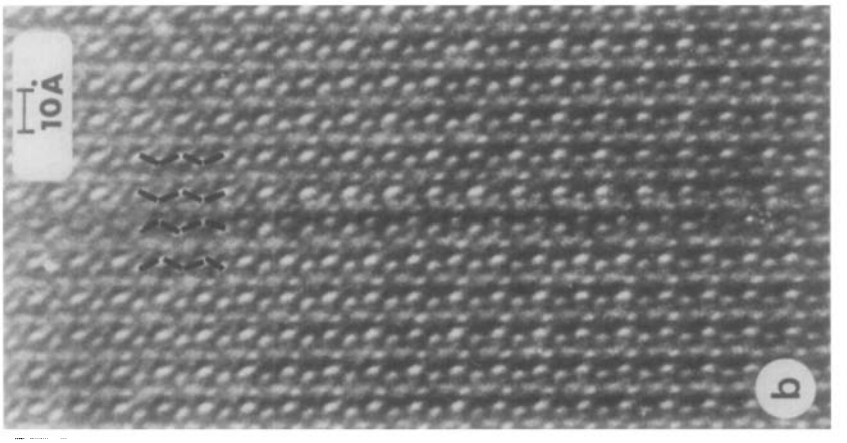

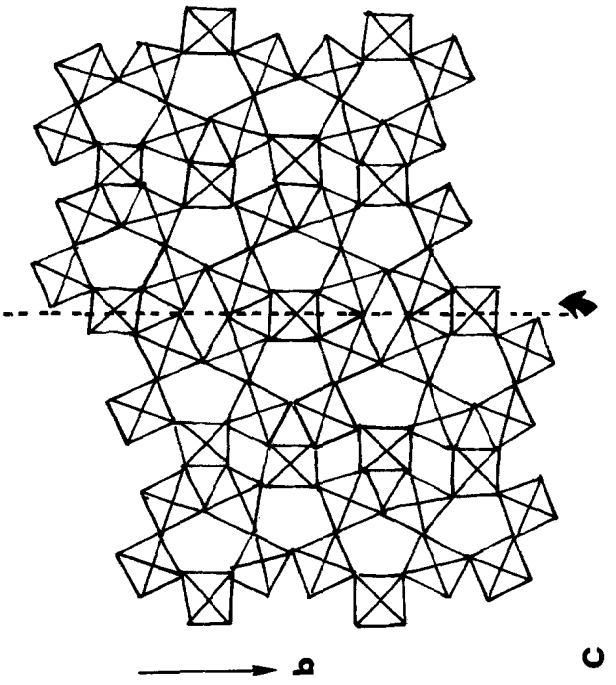

FIG. 9. (a) High-resolution micrograph of a $Ba_{0.15}WO_3$ crystal exhibiting defects. (b) Enlargement of the defect and directions of the zig-zag ribbons. (c) Idealized drawing of the defect.

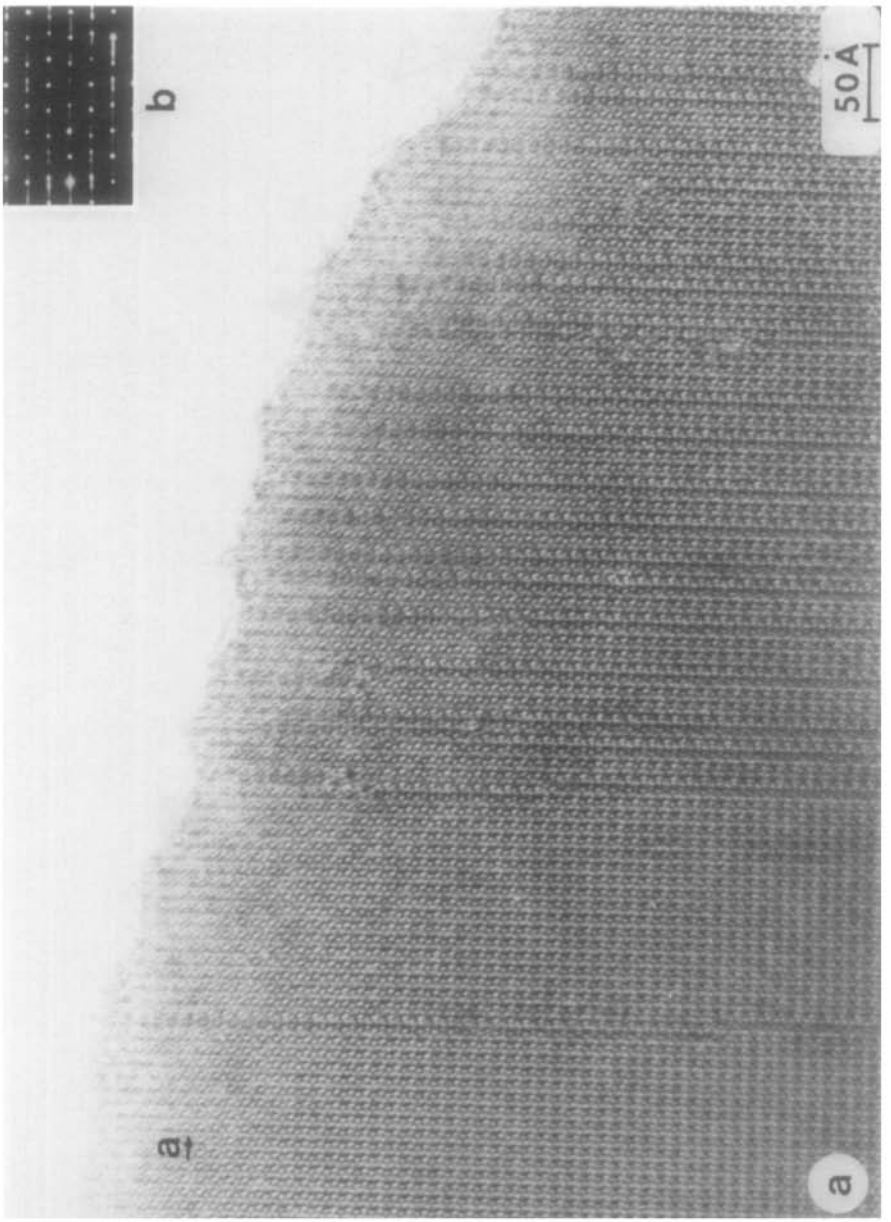

FIG. 10. (a) High-resolution micrograph of a disordered crystal. (b) Electron diffraction pattern.

References

1. A. MAGNELI AND B. BLOMBERG, *Acta Chem. Scand.* **5,** 372 (1951).
2. A. MAGNELI, *Acta Chem. Scand.* **7,** 315 (1953).
3. E. BANKS AND A. GOLDSTEIN, *Inorg. Chem.* **7,** 966 (1968).
4. D. R. WANLASS AND M. J. SIENKO, *J. Solid State Chem.* **12,** 362 (1975).
5. R. J. BOUCHARD AND J. L. GILLSON, *Inorg. Chem.* **7,** 969 (1968).
6. P. E. BIERSTEDT, J. A. BITHER, AND F. J. DARNELL, *Solid State Commun.* **4,** 25 (1966).
7. A. B. SWANSON AND J. S. ANDERSON, *Mater. Res. Bull.* **3,** 149 (1968).
8. PH. LABBE, M. GOREAUD, B. RAVEAU, AND J. C. MONIER, *Acta Crystallogr. B* **34,** 1433 (1978).
9. PH. LABBE, M. GOREAUD, B. RAVEAU, AND J. C. MONIER, *Acta Crystallogr. B* **35,** 1557 (1979).
10. A. MAGNELI, *Ark. Kem.* **1,** 213 (1949).
11. L. KIHLBORG AND A. KLUG, *Chem. Scr.* **3,** 207 (1973).
12. A. HUSSAIN AND L. KIHLBORG, *Acta Crystallogr. A* **32,** 551 (1976).
13. T. EKSTRÖM AND R. J. D. TILLEY, *J. Solid State Chem.* **28,** 259 (1979).
14. L. KIHLBORG, M. SUNDBERG, AND H. HUSSAIN, *Chem. Scr.* **15,** 182 (1980).
15. L. KIHLBORG AND R. SHARMA, *J. Microsc. Spectrosc. Electron.* **7,** 387 (1982).
16. M. GANNE, M. DION, A. VERBAERE, AND M. TOURNOUX, *J. Solid State Chem.* **29,** 9 (1979).
17. A. BENMOUSSA, D. GROULT, F. STUDER, AND B. RAVEAU, *J. Solid State Chem.* **41,** 221 (1982).
18. T. EKSTRÖM AND R. J. D. TILLEY, *J. Solid State Chem.* **24,** 209 (1978).
19. R. STEADMAN, R. J. D. TILLEY, AND I. J. MCCOLM, *J. Solid State Chem.* **43,** 199 (1972).
20. T. EKSTRÖM, M. PARMENTIER, AND R. J. D. TILLEY, *J. Solid State Chem.* **37,** 24 (1981).
21. D. GROULT, M. HERVIEU, AND B. RAVEAU, to be published.
22. D. T. CROMER AND J. T. WABER, *Acta Crystallogr.* **18,** 104 (1965).
23. D. T. CROMER, *Acta Crystallogr.* **18,** 17 (1965).
24. A. J. SKARNULIS, E. SUMMERVILLE, AND L. EYRING, *J. Solid State Chem.* **23,** 59 (1978).
25. C. C. PHAM, J. CHOISNET, AND B. RAVEAU, *Bull. Cl. Sci. Acad. Roy. Belg.* **61,** 1473 (1975).